A Fast Potential Fault Regions Locating Method Used in Inspecting Freight Cars

Zongxiao Zhu
Huazhong University of Science and Technology, Wuhan, China
South-Central University for Nationalities, Wuhan, China
Email: zhuzongxiao@gmail.com

Guoyou Wang
Huazhong University of Science and Technology, Wuhan, China
Email: gywang@mail.hust.edu.cn

***Abstract*—The trouble of freight car detection system (TFDS) is a popular application in Chinese railway today. In this paper, the discrete-point sampling model is further developed to locate potential fault regions in the photos taken by the TFDS. The discrete-point sampling model not only contains the image's region boundary information and region information, but also reflects the transition from region to boundary. The most salient component's contours in samples are drawn by hand and recorded as data templates used for matching in test images. Experimental results show that by components' classification, the method based on this model can classify different types of freight cars' parts universally and locate the potential fault regions more accurately and quickly than regional gray matching or edge matching. The results of anti-noise testing in laboratory and more than two years daily operation at several inspecting stations show that our method has a strong ability to survive with nonlinear deformations, and has a good extensibility to be used with different parts, which meet application demands for the full-automatic inspection system.**

***Index Terms*— TFDS, discrete-point sampling model, components' classification, potential fault regions locating**

I. Introduction

Every day in China, thousands and tens of thousands of freight trains are running on more than 90,000 kilometers railway. The trouble of freight car detection system [1]-[2] （TFDS, official name） is a popular application demanded by the Chinese department of railway now. A TFDS takes 53 photos each freight car with five cameras from sides and bottom as showed in Fig. 1, which means each freight train may have 2,000-3,000 photos according to the number of its boxcars. Four experienced workers will look into all these photos and make judgments whether there are troubles or not in 10 minutes. Our goal is using computer to do the same job with the same accuracy and same speed as those experienced workers do, and change the human-control model to the computer combining with human-control model until the final realization of the complete computer-control model.

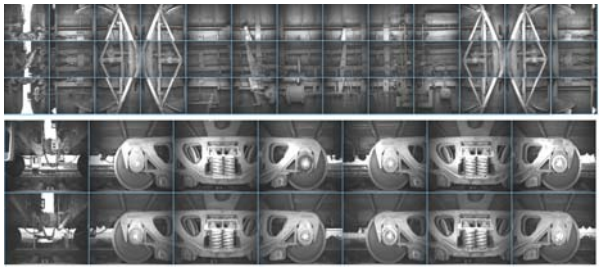

Figure 1. Fifty-three photos from Chinese trouble of freight car detection system.

The key problem in TFDS is how to classify components and locate potential fault regions as quickly as possible. Since China's railway system has been developing rapidly, different kinds of freight cars are running at the same time with a variety of components. Both new and old components, even with the same function, may be designed in different years with several types. Different types of components may have different fault regions in different quantities. The computer fault detection algorithm should first automatically identify the component's type in the freight car, then locate potential fault regions, and detect if there is fault or not in these potential fault regions.

The challenge also comes from the difficulty of components modeling. In TFDS, the status of freight car and photography conditions vary significantly at different inspecting stations such as illumination changes, different weather conditions, varying speed and camera vibration, etc. As a result, the photos of one component type may be quite different in details despite overall similarity. It is impossible to gain identical photos. In this case, if the common regional threshold segmentation or edge extraction algorithms are adopted, irregular and random changes will occur in the regions or edges. So it is very difficult to establish a unified mathematical model representing this type of component.

Manuscript received March 15, 2013.
This work was supported by Wuhan Huamu Science and Technology Company.
Guoyou Wang is the corresponding author.

doi:10.4304/jcp.9.5.1266-1273

Before knowing about TFDS, the railway workers who look over those photos have already been checking out and repairing the faults in freight cars for more than five years. They are quite familiar with those regions with potential faults in various types of components, and they can classify the type of components and locate the region with potential faults as soon as they see the photo. In order to ensure the computer to reach the same detecting ability, many methods have been tried, including line matching[3], edge matching [4], corner point matching[5], SIFT[6] and its variant features [7] matching. However, the classification capacity, locating time and accuracy of these methods are no match for those experienced railway workers. This situation has not been changed until a method based on the discrete-point sampling model [8]-[9] (DPSM) is developed. This model takes advantage of both methods based on object region and boundary, obtaining the boundary information from a yin discrete-point sampling map and regional information from a yang discrete-point sampling map. Yin and yang sampling maps reflect the transitional features from object region to object boundary in the image. Summarized from a large number of images, the transitional features are combined for component structure modeling and component type classification. Better results have been achieved in classifying the component types and locating potential fault regions. Currently, this model has been successfully applied in several freight car stations with TFDS.

This paper is organized as follows. Section 2 briefly introduces the developed discrete-point sampling model. Section 3 presents how the discrete-point sampling model be used to locate the potential fault regions in a TFDS. In Section IV, we describe and discuss the results of our experiments. Section V offers our conclusion.

II. THEORY

A. Discrete-point Sampling

The visual basis for application of the discrete-point is primarily established upon the spatial characteristics of vision, including the cumulative effect in space and the limitation of visual acuity [10]. Visual acuity of human eyes has a certain limit. For instance, based on the optical diffraction principle, a single light spot in a scene will no longer be a single spot when focused on the retina, but a pattern composed of a central bright disk and a series of surrounding dark and bright rings. The width of a fine line on the retina is always larger than 0.0087rad, no matter how fine the original test line is. Under the best light conditions, the best eyes of human beings can only distinguish grids composed of lines with width corresponding to 0.0097-0.011rad on the retina. Considering all these visual features, the major structural information in an image can be conveyed by a series of discrete-point in the image. Human brain can easily combine these discrete points and obtain meaningful information. Different amounts of discrete-point can convey different quantities of information and present the details of the image at different levels, which can be seen

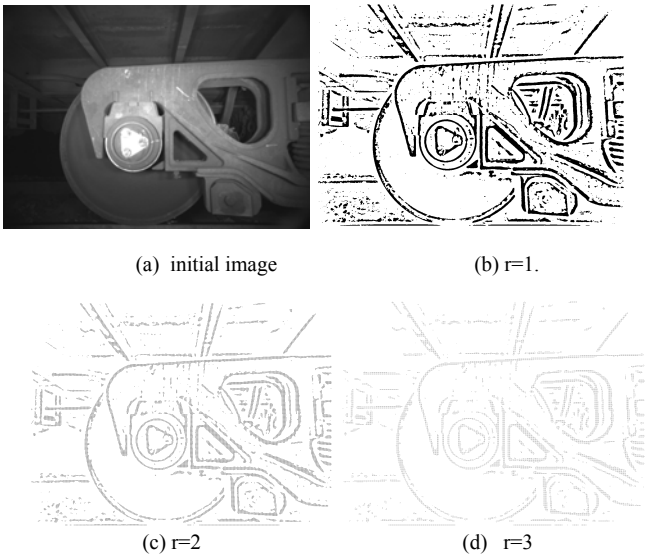

Figure 2. Initial image(1400×1024) and images composed of discrete-point with different sampling radii.

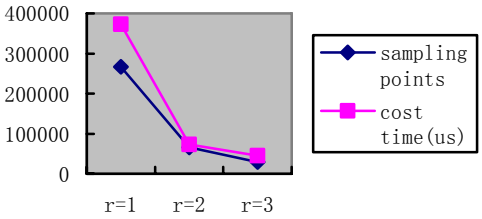

Figure 3. Relationship among sampling radius, sampling points and sampling time.

clearly in Fig. 2. It can be seen that as the sampling radius increases, the detailed information of the image is gradually decreasing, but it is still quite easy for human eyes to locate the wheel. If the current task is wheel locating, Fig. 3 (d) with r=3 can provide sufficient information with 25674 yin pixels, which account for only 2% of the total number of pixels in the original image. Fig. 3 gives the relationship among sampling radius, sampling points and sampling time in Fig.2. As shown in the figure, when sampling radius increases from 1 to 2, the number of sampling points reduces by 75.2%, and sampling time shortens by 80.3%. Taking into account the convenience of grouping, we use r=2 as default sampling radius in our applications.

B. Sampling Model

In this paper, we define yin points are pixels located in the region with uneven brightness, while yang points are pixels located in the region with even brightness. This involves how we perceive brightness contrasts. Our sampling model based on the perception of brightness contrast takes the following two factors into account:

1) The human visual system mainly perceives the changes of brightness rather than brightness itself. The

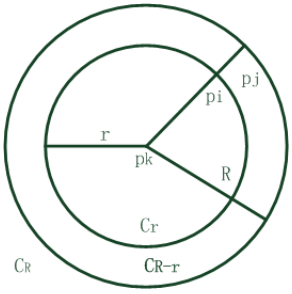

Figure 4. The diagram of discrete-point sampling model.

psychological brightness of a surface is generally determined by the relationship between the brightness of itself and its surroundings. The sampling model should contain such relationship.

2) There are certain limits for human eyes to perceive the change of brightness. Firstly, the brightness difference between two images must be no less than $\triangle B_{min}$, which is the minimum brightness difference perceivable for human eyes. And however the ambient brightness B changes, the ratio $\triangle B_{min}$ /B remains the same and equals to a constant. This constant should be regarded as a threshold in the sampling model to tell whether the discrete point is in a region with even brightness or not.

The second factor is based on the Weber-Fechner Law[11]. The minimum brightness difference perceivable for human eyes $\xi = \triangle B_{min}/B$, is called contrast sensitivity threshold or Weber-Fechner Ratio. Generally, for human eyes, $\xi = 0.005 \sim 0.02$. In case of extremely high or low brightness, ξ can rise up to 0.05. When watching TV, ξ may be larger due to the effects of stray lights. All these can be taken as a reference for the value selection of ξ in the sampling model.

Comprehensively considering the above two factors, a sampling model for discrete points is further developed in this paper, as shown in Fig. 4. In this model, C_r and C_R represent the inner circle and outer circle of concentric circles, and their radiuses are r and R respectively. $R \geq r+1$. C_{R-r} is a concentric ring. pi is the No. i pixel in C_r, and gi is the brightness value of p_i. p_j is the No. j pixel in C_{R-r}, and g_j is the brightness value of p_j. r is chosen as the sampling radius for discrete-point, which means the distance between each sampling point and its 4-neighborhood sampling points is r. The values of r and R are related to the type and size of the object to be detected.

According to the Weber-Fechner Law, the difference between mean brightness of ring region C_{R-r} and mean brightness of inner circular region C_r is the brightness difference in the neighborhood of the center point. This brightness difference divided by the mean brightness of inner circular region C_r is $U(p_k)$, the relative brightness uniformity in the neighborhood of p_k . So the sampling operator for p_k is developed as follows:

$$U(p_k) = \frac{\left| \frac{1}{C_{R-r}} \sum_{p_j \in C_{R-r}} g_j - \frac{1}{C_r} \sum_{p_i \in C_r} g_i \right|}{\frac{1}{C_r} \sum_{p_i \in C_r} g_i} \quad (1)$$

Next, Weber-Fechner Ratio ξ is introduced as a threshold to evaluate the brightness uniformity of p_k's neighborhood, Sampling operator for yin discrete-point:

$$T(p_k) = \begin{cases} 1 & U(p_k) > \xi \\ 0 & U(p_k) \leq \xi \end{cases} \quad (2)$$

Sampling operator for yang discrete-point:

$$T(p_k) = \begin{cases} 1 & U(p_k) < \xi \\ 0 & U(p_k) \geq \xi \end{cases} \quad (3)$$

In applications, the sampling map (yin or yang), sampling radius r and the threshold ξ should be appropriately selected according to the type and size of objects to be detected, and noise level in the image. If the object is a plane, yang sampling map should be choose and Formula (1), (3) should be used for sampling the original image. If the object is a line or a point, yin sampling map should be choose and Formula (1), (2) should be used for sampling the original image. Sampling radius r should be determined by the size of objects. Generally speaking, the larger the size of object to be detected is, the larger the sampling radius is, and the common value of r is 2 in our applications. The threshold ξ to evaluate the brightness uniformity in the neighborhood is affected by the overall noise level of the image. Higher noise level requires larger ξ to restrain noise interference; otherwise, the value of ξ can be smaller, and the common value of ξ is 0.05 in our applications. In practice, there is no need to select the optimal Weber-Fechner Ratio ξ for the human eyes. If the entire photo is too dark to identify the details, ξ can be decreased to increase detailed information, which is contrary to physiological property of human eyes. If the photo has too many details and contains a lot of noise, ξ can be increased to reduce unnecessary information.

III. Application

Based on the DPSM, a new technique is invented to automatically classify the components of freight cars and locate the regions with potential faults. This technique is efficient, accurate, simple and general. This technique can judge the structural type of the component in the image and locate the regions with potential faults in 200~300 ms. Meanwhile, it is applicable to all parts of the freight car, which lays a solid foundation for the further research on automatic fault detection of freight cars. The procedures of this technique are as follows:

Step 1: Select learning samples for all types of components in a certain part of freight cars, and at least one learning sample for each type of component.

Step 2: After careful observation of the yin sampling maps and yang sampling maps from learning samples, some components in these learning samples are selected and their contours are drawn up by hand in their sampling maps. At least one component's contours should be drawn up for each learning sample. The contours are not necessarily continuous or closed. The standard for drawing up the contours of the component is to clearly distinguish the current learning sample from other

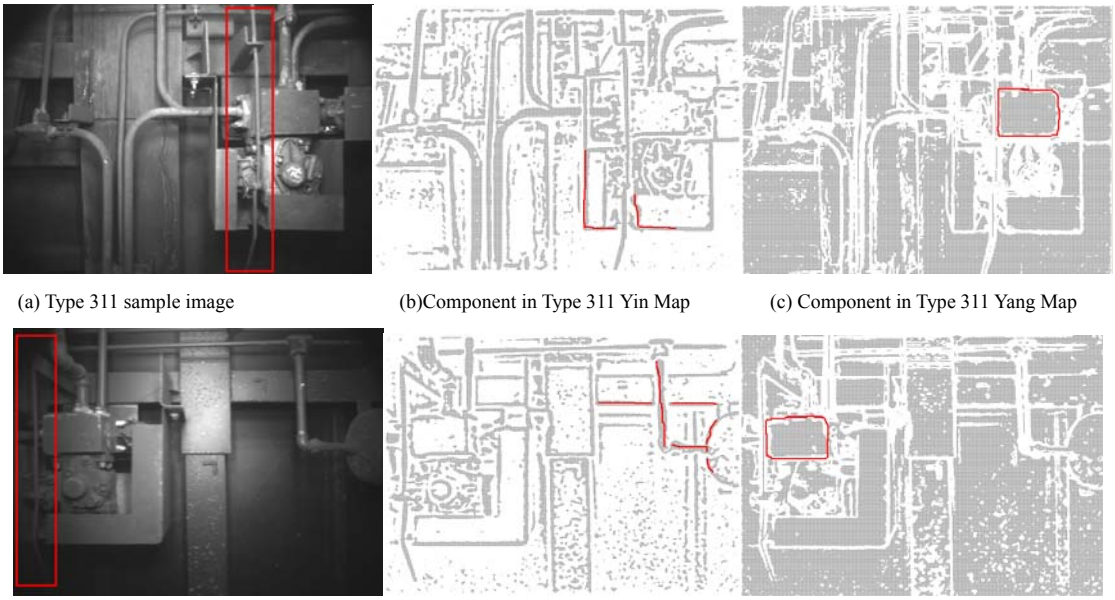

(a) Type 311 sample image (b)Component in Type 311 Yin Map (c) Component in Type 311 Yang Map

(d) Type 312 sample image (e)Component in Type 312 Yin Map (f) Component in Type 312 Yang Map

Figure 5. Contours of the component in Part n_3_1 drawn by hand in yin sampling maps.

learning samples within the same part of freight cars. Fig. 5 shows the contours of the component in Part n_3_1 drawn by hand in yin –yang sampling maps.

Step 3: Store the information about the hand-drawn contours of all components from all learning samples within the same part of freight car in the format of *.ink data file, and prepare the ink data file for this part of freight car. The information stored in *.ink data file mainly includes: yin and yang location sign of each component in each sample, each component's code, the code of the part that the components belong to, the code of structural type that the part belongs to, number of fault regions, serial number of learning sample in the part, coordinates of a component locating point in its learning sample, search radius of component locating point, type of component locating point, key length for component locating and coordinate sequence of component contour points, etc.

Step 4: Select an *.ink data file for a test image according to which part of freight car it shows, and then calculate the yin or yang sampling map of test image using formula 2 or 3 according to the yin and yang location sign of every component in this *.ink data file. Yin and yang sampling maps might be calculated only once for each test image.

Step 5: In the yin or yang sampling map of test image, take the coordinates of component locating point in its learning sample as the search center, search the component locating point in the test image within the search radius of the component locating point according to the type of component locating point and key length for component locating. Only those points that can meet the key length for component locating and correspond to the type of component locating point can be regarded as the potential component locating points in the test image.

Step 6: Load the coordinate sequence of component contour points onto all the potential component locating points of the test image, i.e. map the coordinate sequence of component contour points in the corresponding learning sample into yin or yang sampling map of test image for matching. Suppose N_m is the actual number of matching points, N_{ink} is the number of points in the coordinate sequence of component contour points. If this mapping receives the "response" of yin or yang sampling map, which means there are yin or yang sampling points appearing in the mapping region, then these points will be

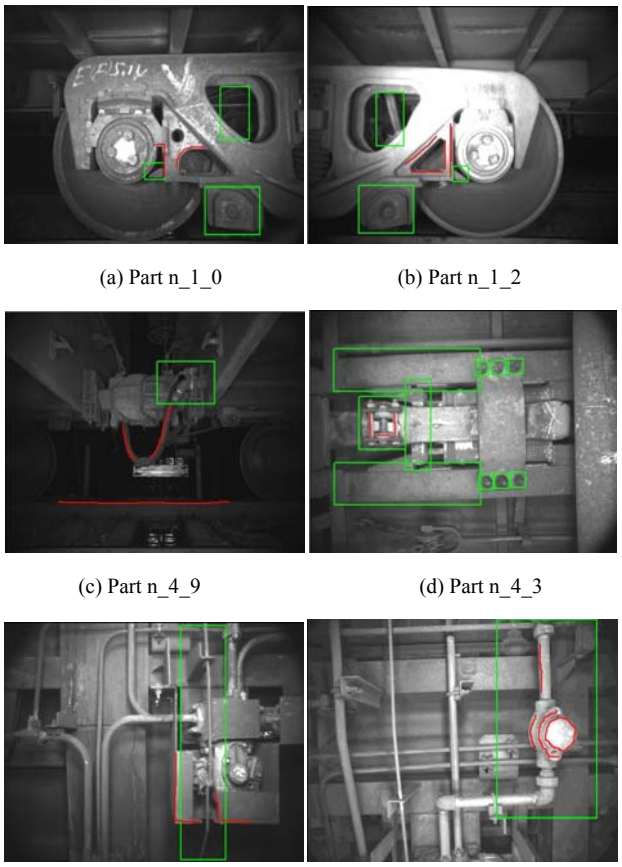

(a) Part n_1_0 (b) Part n_1_2

(c) Part n_4_9 (d) Part n_4_3

(e) Part n_3_1 (f)Part n_3_4

Figure 6. Classification and locating results in different parts of TFDS.

counted as matching points. The total number of matching points N_m divided by the number of points in the coordinate sequence of component contour points N_{ink} is the match ratio of the test image to the contour of this component, as shown in Formula 6:

$$\lambda = \frac{N_m}{N_{ink}} \tag{6}$$

Step 7: Rank the order of the match ratios calculated according to all the coordinate sequences of component contour points. The component type with highest match ratio is most likely to be the component type existing in the test image. Then the part's structural type in the test image can be determined according to the code of the part that this component type belongs to and the code of structural type that the part belongs to.

Step 8: Locating of region with potential faults. After the proper classification of structural type in a certain part of freight car, it becomes easier to locate the regions with potential faults according to its structural type. First, these regions are marked in the above learning samples, and information about the type and location of faults is also recorded in the ink data file that contains the information about components in learning samples. After the component in the test image is located, the location of its regions with potential faults can be confirmed as well. Fig. 6 shows the location of regions with potential faults in different part s.

When preparing the ink files, attention should be paid to the following aspects and the accuracy of classification may be effectively improved:

1. Selecting component types with salient differences;

Based on the visual saliency of human eyes, component types with significant differences should be selected, and the conditions for locating points should be set reasonably, so as to achieve an initial acceptable result of classification and locating.

2. Selecting typical sample image for each type of component;

When selecting learning samples for drawing component contour, pay attention to the representativeness of these sample images, and use the least sample images to ensure the search ranges of locating points can cover all the possible regions and the initial conditions of locating points can be met by most test images except for special ones.

3. Appropriately drawing component with auxiliary structural difference

If there are lots of errors appear when classify two groups of structural types , keep the component's contours with significant difference, and draw contours of another component with auxiliary structural difference, so as to improve the accuracy of classification.

IV. Results and Discussion

In this section, we will compare our method with several classical template matching methods, and we will test its performances in classifying and locating, addressing noise interfering, and performing extensible learning. We will use four experiments, including matching comparison, locating test, noise test and extensibility test. Our test environment utilizes an Intel Core i5-2540 2.60GHz CPU , 4 GB RAM, and VC++2010.

TABLE I
MATCHING COMPARISON RESULTS WITH 743 IMAGES

Methods	Accuracy(%)	Average-time (ms)	Mean	Variance	Size (Bytes)
Gray matching 1	99.46	314.64	0.9753	0.000502	200×160
Gray matching 2	99.73	306.96	0.9568	0.001380	200×160
Gray matching 3	100.00	306.11	0.9925	0.000035	200×160
Edge matching	100.00	6955.88	0.9820	0.000005	190×20
Out method	100.00	154.22	0.9300	0.004109	827×4+3

(a) Initial image (1400×1024); (b) edge map; (c) yin DPSM;

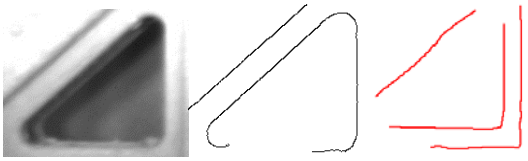

(d) gray template; (e) edge template (f) hand-sketch template.

Figure 7. Three different template matching methods with their templates.

A. Matching Comparison

A total of 744 images with good quality in a component type I of the wheel part as shown in Fig. 3 (a) are selected from a TFDS station. One image is randomly chosen to be the learning sample, as Fig. 7 (a) shows; the chosen image is used to generate an edge map (Fig. 7 (b)) and a yin DPSM (Fig. 7 (c)). The triangular region in the middle of the image is regarded as the salient component; it is marked as component type I of a wheel part, which is used to generate a gray template (Fig. 7 (d)), an edge template (Fig. 7 (e)) and a hand-sketch template (Fig. 7 (f)). All of these three templates are used for matching and locating in the whole range (1400×1024) of the remaining 743 images. All of the best matching areas are cut out as sub-images, to be checked by manual inspection. If there is a whole triangular region, such as Fig. 7 (d) in a sub-image, this matching is correct. If there

TABLE II
REGIONS LOCATING RESULT

Type	151	152	153	154	155	total
Photos' number	773	229	38	33	77	1150
Correct rate(%)	96.9	97.4	97.4	100	96.1	97.04
Time(ms)	231	245	245	284	257	239

is no such triangular region or part of it, then this matching is incorrect.

Table I records, for the three templates, the correct rate, the average time cost, the matching rate's mean and variance and the template's size. The gray template matching uses the cvMatchTemplate function in OpenCV, where schemes 1, 2, and 3 correspond to SQDIFF_NORMED, CCOEFF_NORMED, and CCORR_NORMED, respectively. The template-matching methods that are based on the gray correlation are easily affected by illumination changes or occlusions. Edge matching based on distance transformations [12]-[13] can overcome such effects, while it is computationally expensive and its real-time performance is still not satisfactory. In the method that we proposed in this paper, it costs 90 ms on average to generate a yin DPSM of a whole image, and 65 ms for single hand-sketch template matching. Thus, with half the time of the gray template and 10% of its size, our method not only makes the same matching and positioning result as the gray matching scheme 3 and edge matching do, but also prepares well for subsequent classifications and locating.

B. Test on the Locating of Potential Fault Regions

In this test, the DPSM is applied to locate potential fault regions in wheel-part images from TFDS. 1,150 wheel-part images of the freight car are randomly selected from the total images taken in one day by a test station. These images are used as test samples, including 5 different structural types. Each image is in the original size of 1400×1024. The locating technique based on DPSM is adopted to locate the regions with potential faults in all the wheel images. The accuracy and efficiency of this technique is tested, and the test result is recorded according to the type of the wheel, as shown in TABLE II.

The traditional methods of matching locating by gray-level template or edge template cannot predict the structural types of wheel part, and thereby fail to select the correct template in advance. The locating technique based on DPSM proposed in this paper can simultaneously accomplish such three tasks as detection, locating and classification and reach high efficiency. According to TABLE II., locating accuracy of all five wheel types has reached over 95%, and the average locating accuracy of all the images reaches 97.04%. The average time for one image is equivalent to the time cost by matching with a single gray-level template. Therefore, both classification accuracy and locating efficiency of the technique in this paper can meet the requirements of automatic fault detection of freight cars.

TABLE III
CLASSIFICATION RESULT WITH RANDOM NOISE

SNR	151 (773)	152 (229)	153 (38)	154 (33)	155 (77)	total (1150)
∞	98.06	99.56	100	100	96.10	98.35
25.70	97.67	99.56	97.37	100	97.40	98.09
19.95	98.71	98.69	97.37	96.97	97.40	98.52
17.88	97.93	97.82	78.95	93.94	90.91	96.70
15.02	97.67	93.01	84.21	78.79	84.42	94.87
13.59	92.11	79.91	55.26	45.45	70.13	85.65
13.29	79.56	68.99	28.95	21.21	58.44	72.70

TABLE IV
CLASSIFICATION RESULT WITH RANDOM NOISE

SNR	151 (773)	152 (229)	153 (38)	154 (33)	155 (77)	total (1150)
21.43	99.61	97.82	97.37	100	94.81	98.87
18.50	98.06	60.70	73.68	9.09	20.78	82.09
16.80	97.41	37.12	65.79	3.03	14.29	76.09

TABLE V
RESULTS OF COMPONENT CLASSIFICATIONS IN FIVE PARTS

Parts	n_1_0	n_1_2	n_4_3	n_3_1	n_3_4
primitive types	5	5	5	6	8
no primitive proportion %	0	0	2.6	12.6	11.8
Correct rate %	99.46	99.39	96.21	92.64	91.35

C. Noise Test

After testing millions of TFDS images, it is confirmed that the rapid classification and locating technique based on the DPSM has strong anti- noise capability. In order to analyze the anti- noise capability of image classification and locating method based on DPSM, salt and pepper noise of different signal-to-noise ratios are added to 1150 tested images used in test (a). The classification and locating method based on the DPSM is adopted to classify the images, and experimental results are shown in Table III and Table IV.

According to the experimental result, the classification and locating method based on a DPSM has strong resistance to both random noise and salt-pepper noise. It should be noted that, when the signal-to-noise ratio reduces to a certain degree, Weber-Fechner Ratio ξ can be properly increased to reduce the detailed information and further improve the anti-interference capability of detection system.

D. Extensibility Test

With training, anyone who has experience with a computer can master our hand-sketch shape matching method that is based on a DPSM and can apply it to images of different parts from TFDS. If a new type of component occurs, then we must draw a new hand-sketch template for it, which can be accomplished flexibly by inspectors in each of the TFDS stations according to the actual situations of their recent passing freight cars. Our method has been successfully applied to more than 10

parts in several TFDS stations for more than two years. In the following five-part test, we extract 2000 images for each part randomly from a TFDS, and Fig. 6 shows their classification and locating results. Table IV shows the experimental results of component classifications with mainstream types in five parts of TFDS based on our method. The mainstream types of components refer to the common component types in this part, for which the hand-sketch has been drawn and recorded. Because non-mainstream types refer to some component types that occasionally appear in this part and that differ greatly from the mainstream components, their hand-sketches are not drawn. During classification, those non-mainstream types should be distinguished as a special category, i.e., the category that could not be recognized. However, because of the irregular and wide changes, the non-mainstream types are likely to be detected as mainstream types of components, which lead to errors in the classification results. The experimental results in table IV show that, for parts with small structural changes and without non-mainstream types of components, the accuracy of this classification method can reach over 99.0%; while for parts with complex structure and large proportions of non-mainstream types of components, the accuracy of this classification method decreases to 90%. In this case, the threshold for some false fault alarms should be appropriately decreased, and manual judgments are needed.

V. CONCLUSIONS

The DPSM reflects the transient process from object region to object edge and provides a platform for storing, representing, searching and detecting object structures. To detect the images in a certain part of TFDS is actually to give an overall description of all the image samples in this part. This description not only includes edge information and regional information, but also includes the relative positions of edges and regions and allows the mutual conversion between edges and regions, which may be caused by position deviation, light changes or covered spots. Nevertheless, as long as the component of freight car exists, the transient process from component region to component edge will exist undoubtedly. This transient process is not reflected by a certain pixel or edge, but distributed in a certain region that is not necessarily continuous. In other words, as long as there is a certain region in the yin sampling map or yang sampling map that can contain the contour of a certain component of the freight car, it can be deduced that the original image probably contains this component. Moreover, whenever the components of freight cars are upgraded, the ink data files can be replaced to update the classification and locating algorithm, so this algorithm can serve as an open and standard tool for TFDS. In fact, compiling ink data files is storing knowledge features, the ink files is corresponding to the storage space of knowledge features of freight car components, and mapping the component data in ink files to sampling maps is searching for knowledge features. All these steps are completed based on yin-yang sampling maps. Yin-yang sampling maps can store the knowledge about the point, line or plane objects. Edge graphs and threshold graphs cannot properly demonstrate the knowledge features of the point, line or plane objects in complex and changing backgrounds. DPSM can solve this problem to some extent under certain conditions, provide a platform for object detection to effectively extract knowledge features, and search knowledge features at a very fast speed only in a small storage space. In many cases, accompanied by discrete point grouping algorithm and computing geometric algorithms, the yin-yang sampling maps can replace edge maps or threshold maps as a more efficient and robust model for object detection in a large quantity of images.

ACKNOWLEDGMENT

This work was supported in part by the Natural Science Foundation of China under Grant 60975021.

REFERENCES

[1] Z.H. Liu, D.Y. Xiao and Y.M. Chen, “Displacement fault detection of bearing weight saddle in TFDS based on hough transform and symmetry validation,” in *9th International Conference on Fuzzy Systems and Knowledge Discovery (FSKD)*, pp. 1404-1408, Chongqing, China, May. 2012.

[2] X.D. Yang, L.J. Ye and J.B. Yuan, “Research of Computer Vision Fault Recognition Algorithm of Center Plate Bolts of Train,” in *1st International Conference on Instrumentation, Measurement, Computer, Communication and Control*, pp.978-981, Beijing, China, Oct. 2011.

[3] Wang, Yanxia, Yan Ma, and Qixin Chen. "A Method of Line Matching Based on Feature Points." *Journal of Software* 7.7 (2012): 1539-1545.

[4] H.Z. Wang and J. Oliensis, “Rigid Shape Matching by Segmentation Averaging,” *IEEE Trans. Pattern Anal. Mach. Intell.*, vol. 32, no. 4, pp. 619-635, Apr. 2010.

[5] Yang, Huihua, et al. "An Efficient Vehicle Model Recognition Method."*Journal of Software* 8.8 (2013): 1952-1959.

[6] Gao, Tao, et al. "Feature particles tracking for moving objects." *Journal of Multimedia* 7.6 (2012): 408-414.

[7] Zeng, Lin, et al. "A Self-adaptive and Real-time Panoramic Video Mosaicing System." *Journal of Computers* 7.1 (2012): 218-225.

[8] Zhu, Zongxiao, Guoyou Wang, and Jianguo Liu. "Object detection based on multiscale discrete-point sampling and grouping." *Sixth International Symposium on Multispectral Image Processing and Pattern Recognition*. International Society for Optics and Photonics, YiChang, China,2009.

[9] Zhu, Z., et al., “Fast and Robust 2D-Shape Extraction Using Discrete-Point Sampling and Centerline Grouping in Complex Images”. *Image Processing, IEEE Transactions on*, 2013. 22(12): p. 4762-4774.

[10] Ali, Mohamed Ather and Klyne, M.A., “Vision in Vertebrates”. New York: Plenum Press. 1985, pp. 28.

[11] Jianhong Shen, “On the foundations of vision modeling I. Weber's law and Weberized TV restoration,” Physica D: Nonlinear Phenomena, vol.175, no.3-4, pp. 241-251,2003.

[12] R.G. Caves, P.J. Harley and Q. Shuan, “Matching map features to synthetic aperture radar (SAR) images using template matching,”, *IEEE Trans. Geosci. Remote Sensing*, vol. 30, no.4, pp.680-685, Jul. 1992.

[13] J. Kang and G.Yang, “Fast morphological pyramid matching algorithm based on the Hausdorff distance,” in *2011th IEEE International Conference on Cyber*

Technology in Automation, Control, and Intelligent Systems, IEEE, pp.288-292, KunMing, China, Mar. 2011.

Zongxiao Zhu received the BS degree and the MS degree in electrical and electronic engineering from Xi'an Jiaotong University, Xi'an, China in 2000 and 2003, respectively. He is currently pursuing the Ph.D. degree in control science and engineering at the Institute for Pattern Recognition and Artificial Intelligence, Huazhong University of Science & Technology, Wuhan China.

From 2003 to 2004, he was an engineer with SuZhou Shihlin Electric&Engineering Co., where he was in charge of designing small power converters (on the market in 2004). Since 2004, he has been a faculty of College of computer Science, South-Central University for Nationality (SCUN), Wuhan, China. In 2007, he founded the Information Processing Laboratory for Minority Language (IPLML) in SCUN and began to manage a multidisciplinary research team aiming at using information technology to salvage, protect and broadcast endangered minority cultures. His research interests include image processing, object detection, and endangered minority culture's protection with information technology.

Mr. Zhu is a member ACM and a member of Chinese computer federation (CCF).

Guoyou Wang received BS degree in Electronic Engineering and the MS degree in pattern recognition and intelligent system from Huazhong University of Science and Technology, Wuhan, China in 1988 and 1992, respectively. He is currently a professor with the Institute for Pattern Recognition and Artificial Intelligence, Huazhong University of Science & Technology, Wuhan China. His research interests include image processing, image compression, pattern recognition, artificial intelligence, and machine learning.